1   Research Article
2   29 July 2015
3

4

5   **Werner syndrome helicase modulates G4 DNA-dependent transcription and opposes**

6   **mechanistically distinct senescence-associated gene expression programs**

7

8   Weiliang Tang[1*], Ana I. Robles[2*], Richard P. Beyer[3†], Lucas T. Gray[4†‡], Giang Huong Nguyen[2‡],

9   Junko Oshima[1], Nancy Maizels[1,4,5], Curtis C. Harris[2] and Raymond J. Monnat, Jr.[1,6]

10

11   [1]Department of Pathology, University of Washington, Seattle, WA U.S.A.; [2]Laboratory of Human

12   Carcinogenesis, National Cancer Institute, National Institutes of Health, Bethesda, Maryland,

13   U.S.A; [3]Center for Ecogenetics and Environmental Health, University of Washington, Seattle,

14   WA U.S.A.; [4]Department of Immunology, University of Washington, Seattle, WA U.S.A.;

15   [5]Department of Biochemistry, University of WA, Seattle, WA U.S.A.; [6]Department of Genome

16   Sciences, University of WA, Seattle, WA U.S.A. [*,†] these authors contributed equally. ‡ current

17   address: Allen Institute for Brain Science, Seattle, WA (LTG) and Department of Dermatology,

18   University of Colorado Anschutz Medical College, Aurora, CO 80020 (GHN).

19

20   ***Corresponding authors:*** Ray Monnat MD, Departments of Pathology and Genome Sciences,

21   University of WA, Seattle, WA 98195-7705. Phone: +1.206.616.7392; fax: +1 206.543.3967;

22   email: monnat@u.washington.edu ***or*** Curtis C. Harris, MD, Chief, Laboratory of Human

23   Carcinogenesis, Building 37, National Cancer Institute, National Institutes of Health, Bethesda,

24   MD 20892. Phone: +1.301.496.3111; email: harrisc@nih.gov.

25

26

27 **Abstract**

28 Werner syndrome (WS) is a prototypic heritable adult human progeroid syndrome in which signs

29 of premature aging are associated with genetic instability and an elevated risk of specific types

30 of cancer. We have quantified mRNA and microRNA (miRNA) expression in WS patient

31 fibroblasts, and in WRN-depleted fibroblasts. Genes down-regulated in WS patient fibroblasts

32 were highly enriched in G-quadruplex (G4) DNA motifs. The strength, location and strand

33 specificity of this association provide strong experimental evidence that G4 motifs or motif-

34 dependent G-quadruplexes are bound by WRN in human cells to modulate gene expression.

35 The expression of many miRNAs was perturbed by loss of WRN function. WRN depletion

36 altered the expression of >500 miRNAs. miRNAs linked to cell signaling, genome stability

37 assurance and tumorigenesis were among the small number of these miRNAs that were

38 persistently altered in WS patient fibroblasts. An unexpected and highly distinct finding in WS

39 cells was the coordinate over-expression of nearly all cytoplasmic tRNA synthetases and their

40 associated AIMP proteins. Our results provide new insight into WS pathogenesis, and identify

41 therapeutically accessible mechanisms that may drive disease pathogenesis in WS and in the

42 general population.

43

44 **Introduction**

45 Werner syndrome (WS; OMIM #277700) is an autosomal recessive adult human progeroid

46 syndrome caused by loss of function mutations in the *WRN* RECQ helicase gene (1) that

47 encodes DNA-dependent ATPase, 3'- to -5' helicase and 3'- to -5' exonuclease activities (2, 3).

48 The WS clinical phenotype resembles premature aging: graying and loss of hair, bilateral

49 cataract formation and scleroderma-like skin changes appear in the second decade of life in

50 conjunction with short stature. WS patients are at elevated risk for important, age-associated

51   diseases such as atherosclerosis with myocardial infarction and stroke; cancer; osteoporosis;

52   and diabetes mellitus. Of note, there is no elevated risk for Alzheimer disease or other

53   dementias apart from those associated with vascular disease (4).

54   Cancer and cardiovascular disease are the leading causes of premature death in WS, most

55   often in the fifth or sixth decades of life (4, 5). The cancer risk in WS patients is limited to a small

56   number of specific neoplasms: acral lentiginous melanoma; meningiomas; soft tissue sarcomas;

57   primary bone tumors, chiefly osteosarcomas; follicular thyroid carcinoma; and likely both

58   leukemia and antecedent myelodysplasia (6). Loss of function mutations in two other members

59   of the five member human RECQ helicase gene family, *BLM* and *RECQL4,* respectively cause

60   the cancer predisposition syndromes Bloom syndrome (BS), and Rothmund-Thomson

61   syndrome (RTS) and variants. Both BS and RTS have additional, associated developmental

62   findings (2, 3).

63   Biochemical analyses have identified common biochemical substrates for both the WRN and

64   BLM RECQ helicases. These substrates include forked or bubble DNAs, D- and T-loops,

65   Holliday junctions and G-quadruplex structures (2, 3). G-quadruplexes are stable, non-B-form

66   DNA structures that can be formed from nucleic acids containing G4 motifs of sequence $G_{\geq 3}N_{1-x}$

67    $_xG_{\geq 3}N_{1-x}G_{\geq 3}N_{1-x}G_{\geq 3}$. G4 motifs are highly enriched in rDNA, near transcription start sites (TSSs),

68   at the 5' ends of first introns and in exons and introns of many oncogenes (7). We showed

69   previously that G4 motifs are regulatory targets for the BLM RECQ helicase (8), and for binding

70   by the xeroderma pigmentosum-related helicases XPB and XPD (9). Here we quantify mRNA

71   and miRNA expression in WS patient and WRN-depleted primary fibroblasts. Genes and

72   miRNAs whose expression is modulated by WRN mutation or loss identify potential

73   mechanisms by which WRN may modulate gene expression, and functional pathways that may

74   drive WS pathogenesis and disease risk.

75

76   **Results**

77

78   ***Expression profiling identifies WRN-regulated genes and miRNAs***

79   We quantified and compared mRNA and miRNA expression in WS patient (WS) versus

80   matched control (NM) donor primary fibroblasts, and in isogenic control primary human

81   fibroblasts depleted of WRN (**Table S1, Fig. S1, Fig. S2**). Our choice of fibroblasts was driven

82   by the prominent cutaneous features of WS (4, 10), and by the well-defined WS fibroblast

83   cellular phenotype (11). We used array-based profiling to allow a direct comparison with prior

84   attempts to identify altered gene expression in WS patient or WRN altered cells, nearly all of

85   which used comparable expression analysis platforms (12-15)

86   Principal component analysis (PCA) of expression data showed sample partitioning by

87   genotype for mRNA and miRNA expression, with no additional structure reflecting patient/donor

88   age, gender or passage number (**Fig. 1**). Significant differential mRNA expression, defined by

89   an absolute fold difference of $\geq$1.5 with an FDR of <0.05 versus matched controls, was

90   observed in WS fibroblasts for 628 mRNAs with increased expression and 612 mRNAs with

91   decreased expression (**Table S2**). These cut-offs are identical to our previous analysis of mRNA

92   in BS patient and BLM-depleted cells (8), and were chosen after a sensitivity analysis using

93   different cut-off values (see **Supporting Information** Methods for additional detail). WRN-

94   depleted fibroblasts displayed 839 mRNAs with significant increased expression and 674

95   mRNAs with significant decreased expression *versus* nonspecific (NS)-shRNA-depleted

96   controls (**Table S3**). A total of 281 (or 11.4%) of these mRNAs were common to both WS cells

97   and WRN-depleted fibroblasts, with 198 of these (70%) showing coordinate increased or

98   decreased expression in both cell types (**Fig. 1**; **Table S4**).

99   Differentially expressed miRNAs were identified using criteria identical to our previous

100 analysis of miRNA expression in BS patient and BLM-depleted cells (8): by an absolute fold

101   difference of ≥1.5 and a FDR of <0.10 versus controls. Nineteen miRNAs were differentially

102   expressed in WS *versus* control fibroblasts, and 92 miRNAs in WRN-depleted versus NS-

103   depleted fibroblasts. Ten miRNAs were differentially expressed in WS and in WRN-depleted

104   cells: four displayed coordinate increased expression in both cell types (miR-323a-5p, and miR-

105   632, 636 and 639), while the remaining six displayed increased expression in WS cells and

106   decreased expression in WRN-depleted cells (**Fig. 1; Table S5a**).

107   We also examined expression within each cell type of all miRNAs that could be analyzed

108   using each expression platform. WS cells displayed 23 different miRNAs that were differentially

109   expressed versus matched control donors by the above criteria, with 15 having increased

110   expression and 8 reduced expression (**Table S5b**). A corresponding analysis of WRN-depleted

111   versus NS-depleted cells revealed 543 miRNAs significantly altered using the above criteria,

112   with the vast majority (522 of 543 miRNAs or 96%) showing reduced expression)(**Table S5c**).

113   Perturbed miRNA expression in WRN-depleted cells was remarkably robust, with nearly 2/3 of

114   these miRNAs (328 of 334 or 98%) displaying significant differential expression when we used

115   an absolute fold difference of ≥2.0 and a FDR of <0.05 as cutoffs (**Table S5d**).

116   We used two approaches to determine whether altered miRNA expression might be driving

117   altered mRNA expression and disease-associated pathways in WS patient fibroblasts. First, an

118   experimentally-validated miRNA target genes list was used to determine whether a

119   disproportionate number of miRNA-specific target genes were coordinately and reciprocally

120   altered in expression with their cognate, targeting miRNA (**Table S6**). This analysis identified

121   several miRNAs that might drive differential mRNA expression in WS and/or WRN-depleted

122   cells (**Table S6a**). We also performed a more broadly based search for miRNA-target gene

123   pairs as part of an IPA analysis of miRNA expression. This analysis used miRNA-target pairs

124   from miTarBase, TargetScan and additional experimentally-observed miRNA-target pairs to

125   identify miRNAs and target genes whose expression varied reciprocally, and identified 18

126   miRNAs and 218 target genes linked to specific pathways that may contribute to WS disease

127   pathogenesis or disease risk (**Table S7**).

128

129   *G4 DNA motifs correlated with WRN-dependent differential gene expression*

130   In order to determine whether G4 DNA motifs were correlated with WRN-dependent differential

131   gene expression, we determined the frequency of G4 motifs near the transcription start site

132   (TSS) and 5' end of the first intron of genes differentially expressed in WS and/or WRN-depleted

133   cells. An empirical FDR was calculated by comparing G4 motif frequencies in a set of

134   comparably-sized control gene sets randomly selected from all expressed genes (**Fig. 2**).

135   Genes exhibiting reduced expression in WS fibroblasts were highly enriched in G4 motifs on

136   both DNA strands up- and downstream of the TSS, and at the 5' end of first intron (FDR<0.001).

137   G4 motifs were correlated with increased gene expression in WS cells only at the 5' end of

138   intron 1 (FDR=0.022), and with depletion of G4 motifs in the nontranscribed (NT) strand in the

139   250 bp upstream of the TSS (FDR=0.015)(**Tables S8, S9**).

140   Genes exhibiting reduced expression in WRN-depleted cells were significantly enriched for

141   G4 motifs on the NT strand downstream of the TSS (FDR<0.001), and on both strands at the 5'

142   end of intron 1 (TS, FDR=0.003; NT, FDR<0.001)(**Fig. 2**). Conversely, genes whose expression

143   was increased by WRN depletion lacked G4 motifs on either strand downstream of the TSS

144   (FDR = 0.012), or on the NT strand at the 5' end of intron 1 (FDR < 0.001)(**Tables S10, S11**).

145   These results indicate that G4 DNA motifs near the TSS and at the 5' end of first introns may be

146   physiologic targets for WRN binding leading to altered gene expression in human cells.

147

148   *Molecular functions and pathways altered in WS and WRN-depleted cells*

149   Ingenuity Pathway Analysis (IPA Ingenuity Systems; www.ingenuity.com) and gene set

150   enrichment analysis (GSEA) were used to identify molecular and cellular functions, canonical

151   pathways and networks perturbed in WS patient and WRN-depleted primary fibroblasts (**Table**

152   **1, Tables S12-S14**). Top-ranked functions perturbed in both WS and WRN-depleted cells were

153   'cell growth/proliferation', 'cell death/survival' and 'cell cycle'. 'Cellular development' and 'cell

154   movement' were highly ranked in WS cells, as were 'cellular assembly/organization' and 'DNA

155   replication/recombination/repair' in WRN-depleted cells. Four top-ranked canonical pathways

156   altered in WS fibroblasts involved protein synthesis: tRNA charging, and EIF2, mTOR and

157   'regulation of eIF4 and p70/S6 kinase' signaling. Signaling pathways represented 8 and 7 of the

158   top 10 perturbed pathways in, respectively, WS patient and WRN-depleted fibroblasts with 'aryl

159   hydrocarbon receptor (AHR) signaling' top-ranked in WRN-depleted cells and fifth-ranked in WS

160   patient fibroblasts (**Table 1, Tables S12, S13**). The top-ranked perturbed networks in WS cells

161   were focused on connective tissue biology and disease. These were of considerable interest

162   given the strong cutaneous phenotype and increased risk of connective tissue neoplasms of WS

163   (**Table S12**)(6, 10).

164   Gene set enrichment analysis (GSEA) identified gene sets that contained disproportionate

165   numbers of genes that were differentially expressed in WS and/or WRN-depleted cells (**Table 2,**

166   **Table S14**). Top-ranked C2_CP (Canonical Pathways) gene sets identified by this analysis for

167   WS cells were Reactome tRNA/cytosolic tRNA aminoacylation and KEGG Aminoacyl tRNA

168   biosynthesis (**Table S15**). C3_TFT (Transcriptional Factor Target) gene sets were significantly

169   enriched for 62 binding sites encompassing 66 different TFs in differentially expressed genes

170   WS cells, and for 26 binding sites encompassing 26 TFs in WRN-depleted cells. Binding sites

171   for 7 TFs were enriched in both WS and WRN-depleted cells, together with differential

172   expression of 5 TFs in WS cells and 2 TFs in WRN-depleted cells (**Table S16**). Our G4 motif,

173   IPA and GSEA analysis results collectively suggest that WRN modulates gene expression via a

174   regulatory network that includes G4 DNA elements and TFTs in *cis*, and miRNAs and TFs in

175   *trans*.

176   ***Coordinate upregulation of cytoplasmic tRNA synthetase and AIMP genes in WS***

177   A surprising finding in IPA and GSEA analyses of WS cells was 'tRNA charging' as a top-ranked

178   altered canonical pathway (IPA p-value=1.26E-07) in conjunction with several other pathways

179   that regulate protein synthesis (**Table 1, Table S12**). The tRNA charging pathway consists of

180   genes encoding 19 cytoplasmic and 20 mitochondrial tRNA synthetases (ARSs), 3 ARS-

181   interacting multifunctional proteins (AIMPs) and several phosphatases (Reactome tRNA

182   aminoacylation pathway REACT_15482.3). WS cells displayed significantly increased

183   expression of 15 of the 18 cytoplasmic ARS genes and the 2 AIMP genes included on our array

184   platform (**Fig. 3**). Of note, 'tRNA charging' did not appear among the 100 top-ranked pathways

185   in WRN-depleted cells (IPA p-value=0.29), which displayed increased expression of only 3

186   cytoplasmic ARS genes and AIMP1 in conjunction with reduced expression of 2 ARS genes

187   (**Fig. 3, Table S12**). This pattern of coordinate increased cytoplasmic ARS/AIMP expression

188   was both highly distinctive and statistically significant: WS cells were the top-ranked data set for

189   this expression pattern among 5,474 comparison samples from GSE GEO (Gene Expression

190   Omnibus) data (**Fig. 3**, **Table S17**). Of note, ARS/AIMP expression was not significantly

191   perturbed in recently described human *WRN* knockout embryonal stem cells (ESCs) or in

192   differentiated mesenchymal stem cells (MSCs)(16).

193

194   ***WRN suppresses mechanistically distinct senescence programs***

195   Cellular senescence is a prominent phenotype in both WS patient and WRN-depleted cells (11).

196   We thus determined whether senescence-associated genes and gene sets representing

197   mechanistically distinct senescence pathways were differentially expressed in WS and/or WRN-

198   depleted cells (**Tables S18, S19**). Six gene sets were used: a senescence gene 'superset' (156

199   genes; REACT_169274.2); and gene sets reflecting oncogene-induced senescence (30 genes;

200   REACT_169325.2); oxidative stress-induced senescence (89 genes; REACT_169436.2); DNA

201   damage/telomere stress-induced senescence (58 genes; REACT_169185.2); the senescence-

202   associated secretory phenotype (SASP)(75 genes; REACT_169168.2); and

203   'SASP_components_genes', 81 genes encoding cellular or secreted SASP factors assembled

204   from (17, 18)).

205   GSEA analysis indicated significant enrichment of genes that were differentially expressed

206   in WS and/or WRN-depleted cells in four of these gene sets. Increased gene expression was

207   observed for differentially expressed genes in the 'DNA damage/telomere-induced senescence'

208   gene set (in WS cells), and the 'SASP_components_genes' set (in WRN-depleted cells), with

209   most other genes displaying reduced expression (**Fig. 4**). These results indicate that *WRN*

210   mutation and WRN depletion significantly alter the expression of many genes associated with

211   mechanistically distinct, senescence-associated gene expression programs. Several different

212   senescence-associated pathways included in this analysis, most notably the senescence-

213   associated secretory phenotype (SASP) pathway, may serve as potential drivers of WS cellular

214   and organismal phenotypes.

215   We also looked for significant enrichment for differentially expressed genes (DEGs) in gene

216   expression data recently reported for human *WRN* mutant ESCs and MSCs (16). As

217   anticipated, *WRN* mutant ESCs showed a very low proportion of DEGs across all six

218   senescence-associated gene sets. *WRN* mutant MSCs most closely paralleled WRN-depleted,

219   as opposed to WS patient, cells: MSCs displayed a similar distribution, though lower proportion,

220   of DEGs together with a higher ratio of genes with reduced as opposed to increased expression

221   when compared to WS and WRN-depleted cells (**Fig. S6**).

222

223   ***WRN and BLM regulate distinct sets of target genes***

224   The WRN and BLM human RECQ helicases share many functional similarities including G4

225   motif-dependent gene expression. We thus compared gene expression changes in WS cells

226   with cells from patients with Bloom syndrome (BS). Among 2,179 genes differentially expressed

227   in WS and BS cells, >90% were perturbed only in WS or in BS cells (**Fig. S3**)(8). Among the

228   214 genes differentially expressed in both WS and BS cells, a high fraction (87.4%) displayed

229   coordinate increased or decreased expression and represented a wide range of different

230   functions and pathways (**Table S20**). Common genes exhibiting reduced expression were

231   enriched for G4 motifs on both strands upstream of the TSS (FDR=0.009 and 0.002), and on

232   the NT strand at the 5' end of intron 1 (FDR=0.041). In contrast, genes exhibiting increased

233   expression were enriched in G4 motifs only on the NT strand, upstream of the TSS

234   (FDR=0.025)(**Fig. S4**). A similar pattern was observed in WRN- or BLM-depleted cells: 75% of

235   2,282 differentially expressed genes were altered in only one cell type, and a high proportion of

236   563 common genes (93.1%) displayed coordinate increased or decreased expression (**Table**

237   **S21, Fig. S5**). Genes displaying coordinate decreased expression were enriched in functions

238   that can be tied directly to chromosome structure, DNA metabolism and genome stability

239   maintenance: histone, centromeric protein, cell division cycle (CDC/CDK), mitotic division,

240   replication and repair genes including MCMs, POLD, RAD51 and multiple Fanconi anemia

241   genes)(**Table S21**). A majority of differentially expressed miRNAs in WS or BS cells were

242   unique to one cell type: six of 52 miRNAs shared between WS and/or BS cells were

243   coordinately expressed, as were 10 of 58 miRNAs in WRN- and BLM-depleted cells (**Table**

244   **S22**). These results collectively indicate that WS and BS cells have largely distinct patterns of

245   gene and miRNA expression, though share small subsets of genes that are enriched for G4

246   motifs and coordinately regulated miRNAs.

247

248   **Discussion**

249   We used RNA expression profiling to identify genes and miRNAs that were differentially

250   expressed in cells that lacked WRN RECQ helicase protein function as a result of *WRN*

251   mutations or WRN protein depletion. This experimental design was chosen to unambiguously

252   identify genes and miRNAs whose expression was altered in a WRN-dependent manner; to

253   identify potential mechanisms by which WRN modulates gene expression; to reveal adaptations

254   in gene and miRNA expression in response to acute or prolonged loss of WRN function; and to

255   identify functional pathways that might drive WS pathogenesis and disease risk. This design

256   thus substantially extended previous analyses of gene expression in WS cells (12-15), and in

257   recently reported WRN-mutant ESC and MSC cultures where we have further analyzed

258   reported results (16).

259

260   ***G-quadruplexes are targets for regulation by WRN***

261   Biochemical evidence has long suggested G-quadruplex structures may be targets for the

262   RECQ helicases WRN and BLM. Consistent with this idea, we previously showed that the

263   Bloom syndrome RECQ helicase (and the TFIIH XPB and XPD disease-associated helicases)

264   also modulate transcription in a G4 motif-dependent manner (8, 9). In order to test the

265   hypothesis that WRN may modulate gene expression in human cells in a G4 motif-dependent

266   manner, we determined whether genes with reduced expression in WS cells were highly

267   enriched in G4 motifs both upstream of the transcription start site (TSS), near the exon 1/intron

268   1 boundary and in the first 250 bp of intron 1 on one or both DNA strands (**Fig. 2**). These G4

269   motifs are well-positioned to influence gene expression by altering transcription initiation, RNA

270   Pol II pausing, and pre-mRNA splicing.

271   Our results collectively provide strong evidence that G4 motifs and/or G-quadruplex

272   structures formed from G4 motifs are physiologic targets for transcription regulation in human

273   cells. A simple regulatory model for WRN G4-dependent modulation of gene expression

274   involves WRN binding and unwinding of G-quadruplex structures *in vivo* to facilitate the

275   transcription of G4 motif-rich genes. Further analyses of the G4 motifs in genes differentially

276 expressed in WS, BS or XPB/XPD cells should provide additional insight into G4 motif and G-

277 quadruplex structures that are targeted by specific helicases in human cells.

278

279 ***miRNA expression is strongly perturbed in WRN-depleted cells***

280 WRN is also able to modulate the expression of a remarkably large number of miRNAs. For

281 example, in WRN-depleted cells 543 miRNAs identified using previously published criteria (8)

282 were significantly differentially expressed in WRN-depleted versus NS control cells, with the

283 vast majority of these (96%) displaying reduced expression. Among the small number of

284 persistently altered miRNAs in WS cells, several were identified that may play roles in WS

285 disease pathogenesis (**Tables S5a-d**). For example, over-expression of the miR-181 family

286 have been implicated in leukemogenesis (19), whereas down-regulation of miR-632 and 636

287 have been implicated in myelodysplasia (20). Further analyses of miRNA-target gene pairs also

288 identified genes and canonical pathways altered in conjunction with persistent miRNA

289 expression that may drive WS disease pathogenesis as we had previously observed for Bloom

290 syndrome (8).

291

292 ***WRN regulates disease-associated functional pathways***

293 *WRN* mutation or WRN depletion both altered the expression of genes involved in cell cycle

294 control, growth and proliferation; DNA replication, recombination and repair; and DNA damage

295 checkpoint signaling (**Table 1, Tables S2-4**). These pathways have been mechanistically linked

296 to genomic instability, cell proliferation defects and cellular or organismal senescence (17, 21).

297 WRN also modulates several overlapping, mechanistically distinct senescence-associated

298 gene expression programs. This differs by pathway and cell type (WS versus WRN-depleted;

299 **Fig. 4**), and our analysis identified gene expression changes that could drive both intrinsic,

300 chromatin state-associated as well as secretory aspects of aging. Of note, these senescence-

301 associated gene expression programs were not as strongly perturbed in recently reported WRN

302 mutant human ESC and MSC cells that have been proposed as WS disease models (**Figure**

303 **S6**)(16). It will be important to characterize the stability and phenotype of WRN-mutant MSCs,

304 and to examine gene and miRNA expression changes in this and other cellular models of WS to

305 determine whether they provide good experimental systems to use to investigate cellular, cell

306 lineage- and tissue-specific consequences of WRN loss of function.

307

Coordinate over-expression of tRNA charging genes in WS cells

309 A surprising and unexpected finding in our mRNA expression analyses of WS cells was the

310 coordinate increased expression of nearly all of the cytoplasmic tRNA synthetases (ARSs) and

311 their associated interacting proteins (AIMPs). This gene expression signature was highly

312 distinctive and statistically highly significant, and provides new insight into WS disease

313 pathogenesis mechanisms.

314 WS patient fibroblasts were the top-ranked data set for coordinate increased ARS+AIMP

315 expression among 5,474 samples in 56 GEO Series (GSE) data sets that included a wide range

316 of cancer, non-neoplastic disease and control samples (**Table S17; Fig. 3 and Table S12**).

317 The mechanism(s) responsible for coordinate increased expression remain to be identified:

318 ARS/AIMP expression does not appear to be strongly driven by G4 DNA motif depletion, or by

319 MYC overexpression, which itself requires WRN expression to avoid rapid cellular senescence

320 (22). MYC may, however, be indirectly influencing ARS+AIMP upregulation as we identified

321 activation of the MYC transcription network in WS cells (see **Table S14**). We did identify

322 differential enrichment for specific transcription factor target sites (TFTs) in WS versus WRN-

323 depleted cells (**Table S16**). Further analysis of these TFTs may provide a more detailed

324 understanding of the regulatory network that governs coordinate ARS and AIMP expression in

325 WS cells, and that coordinately regulates ARS/AIMP expression in normal human cells.

326   The coordinate upregulation of ARS+AIMP genes in WS patient fibroblasts provides

327   intriguing new insight into WS disease pathogenesis mechanisms. The cytoplasmic ARS and

328   AIMP proteins are abundant, comparatively long-lived proteins with copy numbers ranging from

329   10^5 to $>10^6$/cell (23, 24). The increased expression of ARS and AIMP genes in WS cells likely

330   represents a parallel increase in corresponding protein copy numbers in WS cells (25-27).

331   Higher steady-state ARS and AIMP copy numbers could, together with altered EIF2, mTOR,

332   and eIF4/S6 kinase pathway signaling, perturb global protein dynamics in WS cells (**Table 1**).

333   Recent work consistent with the idea of altered global protein dynamics in WS include the

334   observation that rapamycin and hydrogen sulfide can reduce protein aggregation, suppress

335   oxidative stress and reduce DNA damage in WS cells (28) and in WRN-depleted fibroblasts

336   (29). Altered translational fidelity, originally analyzed in WS fibroblasts with inconclusive results

337   (see, e.g., (30)), could also be perturbed in WS cells by increased ARS+AIMP expression,

338   persistent stress signaling and altered senescence-associated gene expression (31, 32).

339   The coordinate, increased expression of cytoplasmic tRNA synthetases in WS could also

340   disrupt 'mitonuclear' balance between cytoplasmic and mitochondrial protein synthesis. Few

341   genes are transcribed and translated in the mitochondrion. Despite this, balanced mitonuclear

342   protein synthesis is clearly important for maintaining mitochondrial function and appears to be

343   actively maintained by a regulatory network involving oxidative phosphorylation status, the

344   mitochondrial unfolded protein response (UPR[mt]) and NAD+/Sir2/Foxo-dependent signaling.

345   This system can also, in some systems, modulate longevity and senescence (33, 34).

346   A third, intriguing mechanism by which increased ARS and AIMP expression could promote

347   WS disease pathogenesis is via 'non-canonical' functions in addition to tRNA charging. These

348   non-canonical functions involve specific ARS and AIMP proteins, ARS protein splice isoforms

349   (35) or proteolytic cleavage fragments, and modulate multiple disease-related metabolic,

350   developmental, angiogenic, tumorigenic, immune and inflammatory pathways (36). The

351   coordinate upregulation of many ARS and AIMP genes and their associated non-canonical

352   functions provides a mechanistically appealing—if provocative—explanation for the pleiotropic

353   organismal phenotype of WS.

354

355   ***Potential therapeutic implications***

356   Further testing the mechanistic ideas outlined above should advance our understanding of

357   WS disease pathogenesis, and may reveal therapeutically accessible pathways that could be

358   targeted both in WS patients and the general population. Global protein dynamics and

359   translational fidelity in WS could be profitably reinvestigated using sensitive, quantitative global

360   profiling assays (25-27, 31, 37, 38). Altered protein dynamics and/or mitonuclear balance, if

361   identified, could be targeted with rapamycin (39) or resveratrol (40). Additional small molecules

362   could also be used to increase NAD+ levels (e.g., PARP-1 inhibitors, nicotinamide and

363   nicotinamide riboside)(41); induce the UPR[mt] (doxycycline (33)); or activate SIRT1 (e.g.,

364   resveratrol and other small molecule activators (40)). Resveratrol itself may act via both SIRT1

365   and tRNA synthetase/PARP-1 pathways (40, 42). Many of these agents have immediate

366   therapeutic potential, as they are or can be used in the clinic, and thus could be useful both in

367   the care of WS patients and in the modulation of age-associated disease pathways revealed by

368   and shared in common between WS and normal aging.

369

370   ***Summary***

371   Werner syndrome, the canonical human adult progeroid syndrome, is a remarkable example

372   of a Mendelian disease that perturbs many aging and age-associated disease pathways (21).

373   Our results provide the first systematic analysis of miRNA expression in WS, and substantially

374   extend prior analyses of gene expression in WS cells (12-15) and in human stem cell models

375   (16). We identified the outline of a WRN-dependent gene expression regulatory network that

376   includes G4 DNA motifs and transcription factor target sites (TFTs) in *cis,* together with miRNAs

377   and TFs in *trans.* Functional pathways linked by this network provide new insight into WS

378   pathogenesis, and may identify new ways to modulate aging and age-associated disease risk in

379   WS patients and potentially in normal individuals (18, 21).

380

381   **Materials and Methods** (see also Methods in *Supporting Information* for additional detail and

382   methods references).

383

384   **Cells.** Primary human skin fibroblast strains (**Table S1**) from 4 mutation-typed WS patients

385   (mean age 33.5 years, median age 33 years) or from 10 age- and gender-matched control

386   donors (mean age 30.2 years, median age 28 years) were obtained from the Coriell Cell

387   Repositories (Camden, NJ, USA). Control human primary fibroblast strain 82-6 was isolated as

388   previously described (8), and WRN was depleted by lentiviral *WRN*-specific shRNA expression

389   and verified by Western blot (**Figs. S1, S2**).

390

391   **mRNA and miRNA expression profiling.** Whole genome transcript exon profiling and miRNA

392   profiling were performed on Affymetrix GeneChip Human Exon 1.0 ST (Affymetrix, Santa Clara,

393   CA) arrays and a custom miRNA microarray or Nanostring nCounter, and differentially

394   expressed genes and miRNAs identified as previously described (8). Expression profiling data

395   are archived under GEO accession number GSE62877.

396

397   **RNA expression analyses.** Principal component analysis (PCA), Ingenuity pathway and gene

398   set enrichment analyses were all performed as previously described (8). Gene Set Enrichment

399   Analyses (GSEA) used all C1-C7 gene sets in the Molecular Signature Database version 4.0.

400   miRTarBase was used to identify experimentally validated gene targets of miRNAs differentially

401   expressed in WS and WRN-depleted cells as previously described (8), and differentially

402   expressed miRNAs were used to seed IPA analysis of miRNA targets and pathways. G4 motifs

403   were located in hg19 using Quadparser , then analyzed for their association with genes

404   differentially regulated in WS or WRN-depleted cells as previously described (8). GSEA was

405   used to determine whether differentially expressed genes were enriched in 6 senescence-

406   associated gene sets (**Figure S6**, **Tables S18 and S19**), and to analyze the uniqueness and

407   statistical significance of coordinate, increased ARS and AIMP expression in 5,474 samples

408   contained in 56 GEO Series (GSE) data sets. GSEA p-values were calculated for three

409   alternative expression hypotheses (up, down, or mixed).

410

411   **Acknowledgments**

Author contributions

426

427 **Study design:** WLT, AR, RPB, LTG, GHN, CCH and RJMJr. **Experiments and data**

428 **interpretation:** WLT, AR, RPB, LTG, GHN, NM, JO, CCH and RJMJr. **Manuscript writing,**

429 **Figures, Tables and Supporting Information:** WLT, AR, RPB, LTG, GHN, NM, JO, CCH and

430 RJMJr.

431

432 **References**

433 1. Yu CE, Oshima J, Fu YH, Wijsman EM, Hisama F, Ouais S, et al. Positional cloning of the

434 Werner's syndrome gene. Science. 1996;272:258-62. DOI:10.1126/science.272.5259.258.

435 2. Croteau DL, Popuri V, Opresko PL, Bohr VA. Human RecQ helicases in DNA repair,

436 recombination, and replication. Annu Rev Biochem. 2014;83:519-52. Epub 2014/03/13. DOI:

437 10.1146/annurev-biochem-060713-035428.

438 3. Sidorova JM, Monnat Jr RJ. Human RECQ helicases: roles in cancer, aging, and inherited

439 disease. Advances in Genomics and Genetics. 2015;5:19-33. DOI: 10.2147/AGG.S54078.

440 4. Epstein CJ, Martin GM, Schultz AL, Motulsky AG. Werner's syndrome: A review of its

441 symptomatology, natural history, pathologic features, genetics and relationship to the natural

442 aging process. Medicine. 1966;45:177-221.

443 5. Goto M, Ishikawa Y, Sugimoto M, Furuichi Y. Werner syndrome: A changing pattern of

444 clinical manifestations in Japan (1917-2008). BioScience Trends. 2013;7(1):13-22. DOI:

445 10.5582/bst.2013.v7.1.13.

446 6. Lauper JM, Krause A, Vaughan TL, Monnat RJ, Jr. Spectrum and risk of neoplasia in

447 Werner syndrome: A systematic review. PLoS ONE. 2013;8(4):e59709. DOI:

448 10.1371/journal.pone.0059709.

449 7. Maizels N, Gray LT. The G4 genome. PLoS Genet. 2013;9(4):e1003468. DOI:

450 10.1371/journal.pgen.1003468.

451   8. Nguyen GH, Tang W, Robles AI, Beyer RP, Gray LT, Welsh JA, Schetter AJ, Kumamoto K,

452   Wang XW, Hickson ID, Maizels N, Monnat RJ Jr, Harris CC. Regulation of gene expression

453   by the BLM helicase correlates with the presence of G-quadruplex DNA motifs. Proceedings

454   of the National Academy of Sciences. 2014;111(27):9905-10. DOI:

455   10.1073/pnas.1404807111.

456   9. Gray LT, Vallur AC, Eddy J, Maizels N. G quadruplexes are genomewide targets of

457   transcriptional helicases XPB and XPD. Nature Chem Biol. 2014;10(4):313-8. DOI:

458   10.1038/nchembio.1475.

459   10. Hatamochi A. Dermatological features and collagen metabolism in Werner syndrome. In:

460   Goto M, Miller RW, editors. *From Premature Gray Hair to Helicase-Werner Syndrome:*

461   *Implications for Aging and Cancer.* Tokyo: Japan Scientific Societies Press; 2001. p. 51-9.

462   11. Martin GM, Sprague CA, Epstein CJ. Replicative life-span of cultivated human cells. Effects

463   of donor's age, tissue, and genotype. Laboratory Investigation. 1970;23:86-92.

464   12. Choi D, Whittier PS, Oshima J, Funk WD. Telomerase expression prevents replicative

465   senescence but does not fully reset mRNA expression patterns in Werner syndrome cell

466   strains. The FASEB Journal. 2001;15(6):1014-20. DOI: 10.1096/fj.00-0104com.

467   13. Kyng KJ, May A, Kolvraa S, Bohr VA. Gene expression profiling in Werner syndrome closely

468   resembles that of normal aging. Proceedings of the National Academy of Sciences.

469   2003;100(21):12259-64. DOI: 10.1073/pnas.2130723100.

470   14. Johnson JE, Cao K, Ryvkin P, Wang LS, Johnson FB. Altered gene expression in the

471   Werner and Bloom syndromes is associated with sequences having G-quadruplex forming

472   potential. Nucleic Acids Research. 2010;38(4):1114-22. DOI: 10.1093/nar/gkp1103.

473   15. Cheung H-H, Liu X, Canterel-Thouennon L, Li L, Edmonson C, Rennert O. Telomerase

474   protects Werner syndrome lineage-specific stem cells from premature aging. Stem Cell

475   Reports. 2014;2(4):534-46. DOI: 10.1016/j.stemcr.2014.02.006.

476 16. Zhang W, Li J, Suzuki K, Qu J, Wang P, Zhou J, Liu X, Ren R, Xu X, Ocampo A, Yuan T,

477   Yang J, Li Y, Shi L, Guan D, Pan H, Duan S, Ding Z, Li M, Yi F, Bai R, Wang Y, Chen C,

478   Yang F, Li X, Wang Z, Aizawa E, Goebl A, Soligalla RD, Reddy P, Esteban CR, Tang F, Liu

479   GH, Belmonte JC. A Werner syndrome stem cell model unveils heterochromatin alterations

480   as a driver of human aging. Science. 2015;348 (6239):1160-3.

481   DOI:10.1126/science.aaa1356.

482 17. Campisi J. Aging, cellular senescence, and cancer. Annual Review of Physiology.

483   2013;75(1):685-705. DOI: 10.1146/annurev-physiol-030212-183653.

484 18. Tchkonia T, Zhu Y, van Deursen J, Campisi J, Kirkland JL. Cellular senescence and the

485   senescent secretory phenotype: therapeutic opportunities. The Journal of Clinical

486   Investigation. 2013;123(3):966-72. DOI: 10.1172/JCI64098.

487 19. Su R, Lin HS, Zhang XH, Yin XL, Ning HM, Liu B, Zhai PF, Gong JN, Shen C, Song L, Chen

488   J, Wang F, Zhao HL, Ma YN, Yu J, Zhang JW.. MiR-181 family: regulators of myeloid

489   differentiation and acute myeloid leukemia as well as potential therapeutic targets.

490   Oncogene. 2015;34(25):3226-39. DOI: 10.1038/onc.2014.274.

491 20. Erdogan B, Facey C, Qualtieri J, Tedesco J, Rinker E, Isett RB, Isett RB, Tobias J, Baldwin

492   DA, Thompson JE, Carroll M, Kim AS. Diagnostic microRNAs in myelodysplastic syndrome.

493   Experimental Hematology. 2011;39(9):915-26.e2. DOI: 10.1016/j.exphem.2011.06.002.

494 21. Kennedy BK, Berger SL, Brunet A, Campisi J, Cuervo AM, Epel ES, Cuervo AM, Epel ES,

495   Franceschi C, Lithgow GJ, Morimoto RI, Pessin JE, Rando TA, Richardson A, Schadt EE,

496   Wyss-Coray T, Sierra F. Geroscience: linking aging to chronic disease. Cell.

497   2014;159(4):709-13. DOI: 10.1016/j.cell.2014.

498

499

500   22. Grandori C, Wu KJ, Fernandez P, Ngouenet C, Grim J, Clurman BE, Moser MJ, Oshima J,

501   Russell DW, Swisshelm K, Frank S, Amati B, Dalla-Favera R, Monnat RJ Jr. Werner

502   syndrome protein limits MYC-induced cellular senescence. Genes and Development.

503   2003;17(13):1569-74. DOI: 10.1101/gad.1100303.

504   23. Beck M, Schmidt A, Malmstroem J, Claassen M, Ori A, Szymborska A, Ori A, Szymborska

505   A, Herzog F, Rinner O, Ellenberg J, Aebersold R. The quantitative proteome of a human cell

506   line. Molecular Systems Biology. 2011;7(1). DOI: doi: 10.1038/msb.2011.82.

507   24. Nagaraj N, Wisniewski JR, Geiger T, Cox J, Kircher M, Kelso J, Pääbo S, Mann M. Deep

508   proteome and transcriptome mapping of a human cancer cell line. Molecular Systems

509   Biology. 2011;7(1). DOI: 10.1038/msb.2011.81.

510   25. Li JJ, Bickel PJ, Biggin MD. System wide analyses have underestimated protein

511   abundances and the importance of transcription in mammals. PeerJ. 2014;2:e270. DOI:

512   doi.org/10.7717/peerj.270.

513   26. Battle A, Khan Z, Wang SH, Mitrano A, Ford MJ, Pritchard JK, Gilad Y. Impact of regulatory

514   variation from RNA to protein. Science. 2015;347(6222):664-7.

515   DOI:10.1126/science.126079.

516   27. Jovanovic M, Rooney MS, Mertins P, Przybylski D, Chevrier N, Satija R, Rodriguez EH,

517   Fields AP, Schwartz S, Raychowdhury R, Mumbach MR, Eisenhaure T, Rabani M, Gennert

518   D, Lu D, Delorey T, Weissman JS, Carr SA, Hacohen N, Regev A. Dynamic profiling of the

519   protein life cycle in response to pathogens. Science. 2015;347(1259038)

520   DOI:10.1126/science.1259038.

521   28. Talaei F, van Praag VM, Henning RH. Hydrogen sulfide restores a normal morphological

522   phenotype in Werner syndrome fibroblasts, attenuates oxidative damage and modulates

523   mTOR pathway. Pharmacological Research. 2013;74(0):34-44. DOI:

524   10.1016/j.phrs.2013.04.011.

525   29. Saha B, Cypro A, Martin GM, Oshima J. Rapamycin decreases DNA damage accumulation

526   and enhances cell growth of WRN-deficient human fibroblasts. Aging Cell. 2014;13(3):573-

527   5. DOI: 10.1111/acel.12190.

528   30. Harley CB, Pollard JW, Chamberlain JW, Stanners CP, Goldstein S. Protein synthetic errors

529   do not increase during aging of cultured human fibroblasts. Proceedings of the National

530   Academy of Sciences. 1980;77(4):1885-9. PMCID: PMC348613.

531   31. Ribas de Pouplana L, Santos MAS, Zhu J-H, Farabaugh PJ, Javid B. Protein mistranslation:

532   friend or foe? Trends in Biochemical Sciences. 2014;39(8):355-62. DOI:

533   10.1016/j.tibs.2014.06.002.

534   32. Lee JY, Kim DG, Kim B-G, Yang WS, Hong J, Kang T, Oh YS, Kim KR, Han BW, Hwang BJ,

535   Kang BS, Kang MS, Kim MH, Kwon NH, Kim S. Promiscuous methionyl-tRNA synthetase

536   mediates adaptive mistranslation to protect cells against oxidative stress. Journal of Cell

537   Science. 2014;127(19):4234-45. DOI: 10.1242/jcs.152470.

538   33. Mouchiroud L, Houtkooper RH, Moullan N, Katsyuba E, Ryu D, Cantó C, Mottis A, Jo YS,

539   Viswanathan M, Schoonjans K, Guarente L, Auwerx J. The NAD(+)/sirtuin pathway

540   modulates longevity through activation of mitochondrial UPR and FOXO signaling. Cell.

541   2013;154(2):430-41. DOI: 10.1016/j.cell.2013.06.016.

542   34. Bennett CF, Vander Wende H, Simko M, Klum S, Barfield S, Choi H, Pineda VV, Kaeberlein

543   M. Activation of the mitochondrial unfolded protein response does not predict longevity in

544   Caenorhabditis elegans. Nature Communications. 2014;5. DOI: 10.1038/ncomms4483.

545   35. Lo W-S, Gardiner E, Xu Z, Lau C-F, Wang F, Zhou JJ, Zhou JJ, Mendlein JD, Nangle LA,

546   Chiang KP, Yang XL, Au KF, Wong WH, Guo M, Zhang M, Schimmel P. Human tRNA

547   synthetase catalytic nulls with diverse functions. Science. 2014;345(6194):328-32. DOI:

548   10.1126/science.1252943.

549   36. Guo M, Schimmel P. Essential nontranslational functions of tRNA synthetases. Nature

550   Chem Biol. 2013;9(3):145-53. DOI: 10.1038/nchembio.1158.

551   37. Ingolia NT. Ribosome profiling: new views of translation, from single codons to genome

552   scale. Nature Rev Genet. 2014;15(3):205-13. DOI: 10.1038/nrg3645.

553   38. Li G-W, Burkhardt D, Gross C, Weissman JS. Quantifying absolute protein synthesis rates

554   reveals principles underlying allocation of cellular resources. Cell. 2014;157(3):624-35. DOI:

555   10.1016/j.cell.2014.02.033.

556   39. Huang K, Fingar DC. Growing knowledge of the mTOR signaling network. Seminars in Cell

557   & Developmental Biology. 2014;36(0):79-90. DOI: 10.1016/j.semcdb.2014.09.011.

558   40. Sinclair DA, Guarente L. Small-molecule allosteric activators of sirtuins. Annual Review of

559   Pharmacology and Toxicology. 2014;54(1):363-80. DOI: 10.1146/annurev-pharmtox-

560   010611-134657.

561   41. Scheibye-Knudsen M, Mitchell SJ, Fang EF, Iyama T, Ward T, Wang J, Wang J, Dunn CA,

562   Singh N, Veith S, Hasan-Olive MM, Mangerich A, Wilson MA, Mattson MP, Bergersen LH,

563   Cogger VC, Warren A, Le Couteur DG, Moaddel R, Wilson DM 3rd, Croteau DL, de Cabo R,

564   Bohr VA. A high-fat diet and NAD+ activate Sirt1 to rescue premature aging in Cockayne

565   syndrome. Cell Metabolism. 2014;20(5):840-55. DOI: 10.1016/j.cmet.2014.10.005.

566   42. Sajish M, Schimmel P. A human tRNA synthetase is a potent PARP1-activating effector

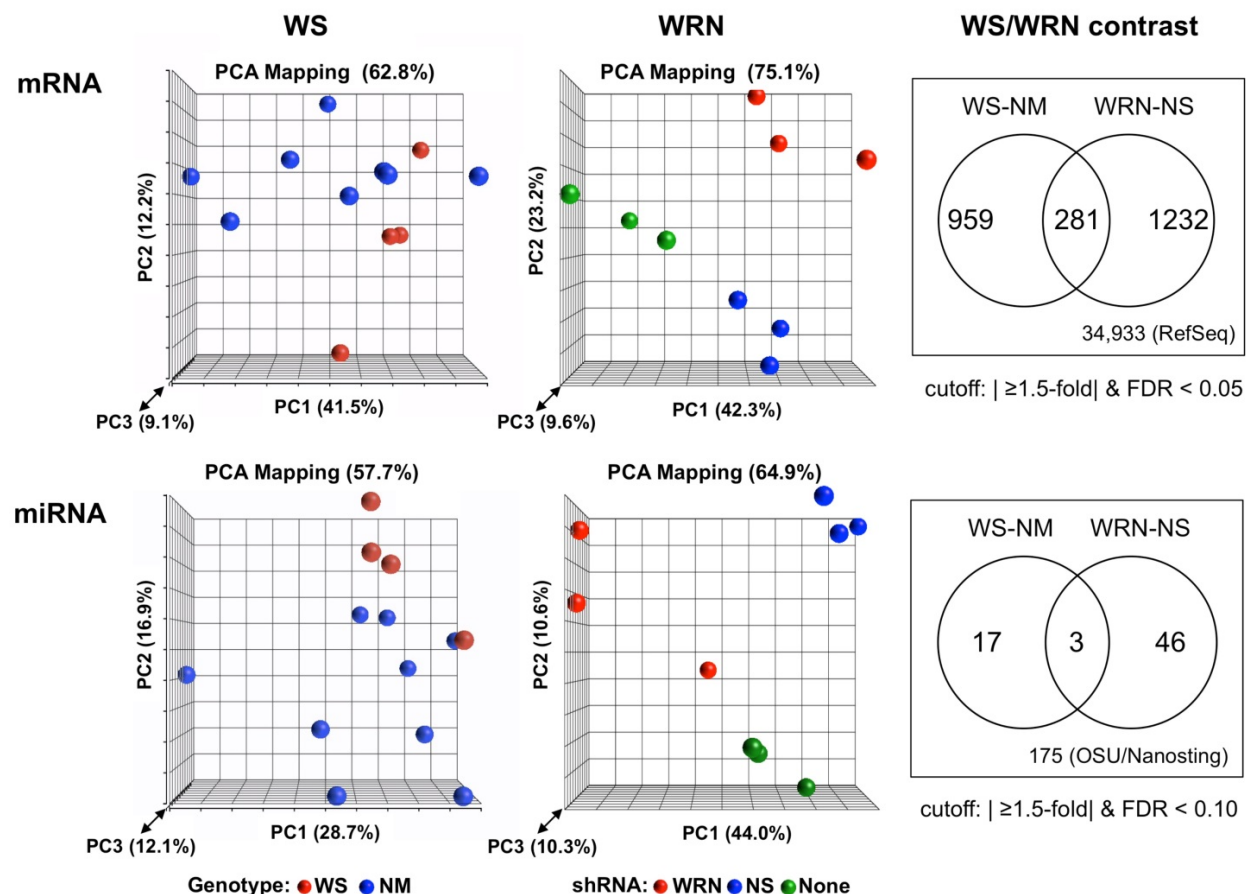567   target for resveratrol. Nature. 2015;519(7543):370-3. DOI: 10.1038/nature14028.

Figure 1. mRNA and miRNA expression patterns distinguish WS and WRN-depleted cells from comparable controls. Principal component analyses (PCA) of mRNA expression (top row) and miRNA expression (bottom row) in Werner syndrome patient (WS, red) and matched control donor (NM, blue) cells, and in WRN-depleted (WRN, red), nonspecific scrambled shRNA treated (NS, blue), and untreated (None, green) cells. Venn diagrams (last column) depict genes (top) and miRNAs (bottom) with significantly altered expression in WS patient or WRN-depleted human primary fibroblasts.
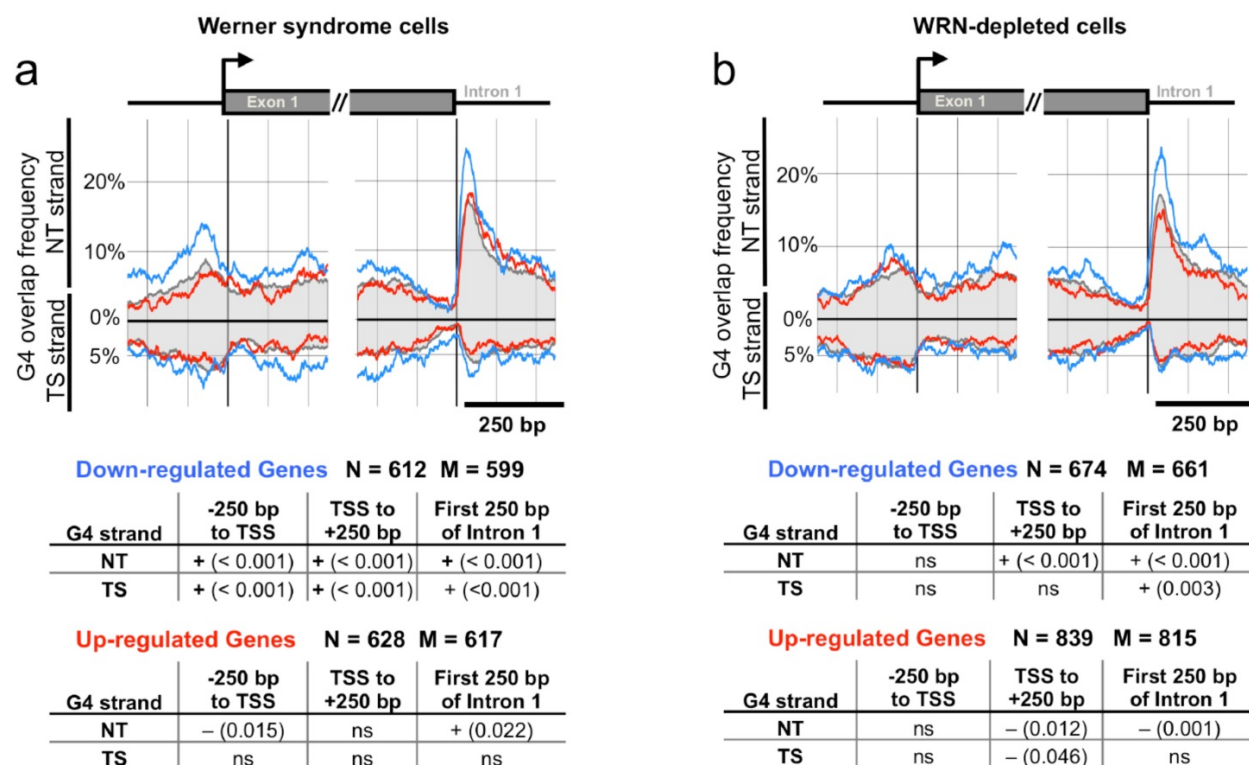
Fig. 2. Enrichment of G4 DNA motifs near TSSs and exon 1/intron 1 boundaries of genes exhibiting differential expression in WS or WRN-depleted human fibroblasts. G4 motif frequencies as a function of location in genes exhibiting differential regulation in (a) WS patient cells or in (b) WRN-depleted control fibroblasts. G4 motif counts relative to the transcription start site (TSS) are shown for the non-transcribed (NT) and transcribed (TS) strand of genes with decreased (blue line) or increased (red line) expression, versus average G4 motif frequencies (gray shaded area) for all genes surveyed. Bottom panel indicates FDRs of observed G4 motif frequencies versus randomly selected control gene sets. N = gene accessions in DEG table; M = number of matching TSS locations from gene location tables; ns: non-significant (FDR>0.05).
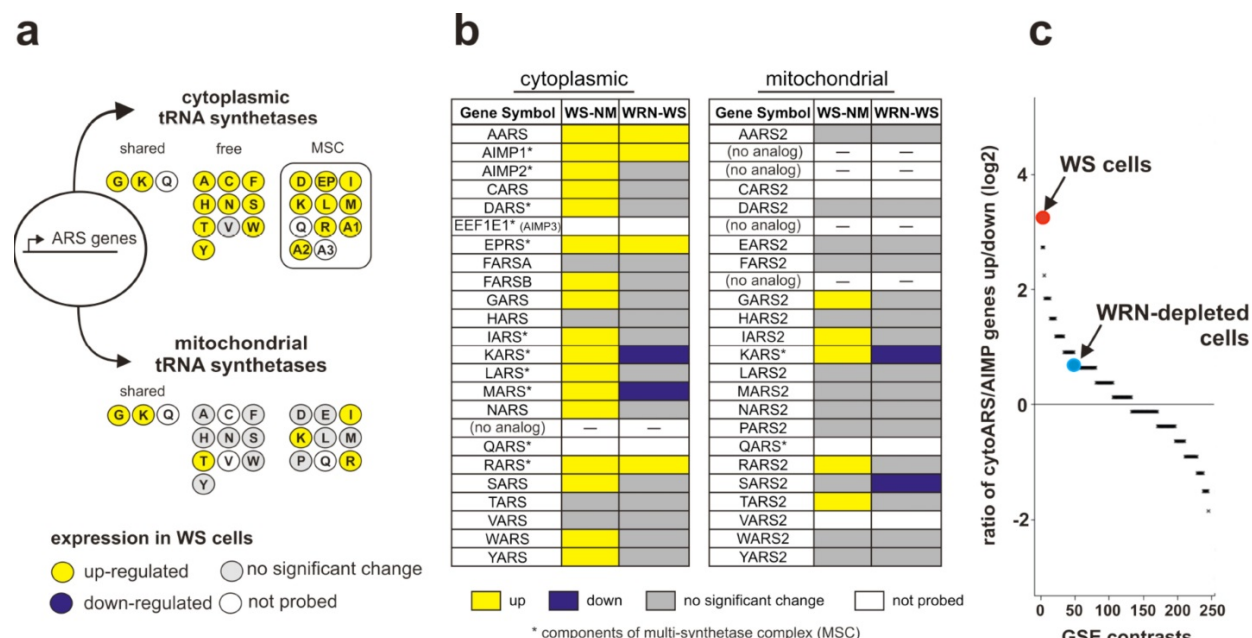
Fig. 3. WS cells display increased expression of many cytoplasmic tRNA synthetase and AIMP genes. (a) tRNA synthetase and AIMP proteins are nuclear-encoded and partitioned to the cytoplasm or mitochondrion with three shared (GARS, KARS and QARS). Eleven ARS+AIMP proteins form a cytoplasmic multisynthase complex (MSC). Individual proteins are represented by circles with single letter amino acid or AIMP number labels. Shading indicates expression in WS cells. (b) ARS/AIMP expression in WS (WS-NM) and WRN-depleted (WRN-NS) cells. (c) ARS+AIMP upregulation ratio in WS and WRN-depleted cells versus 56 GEO Series (GSE) data sets (see *SI Materials and Methods* for additional detail).
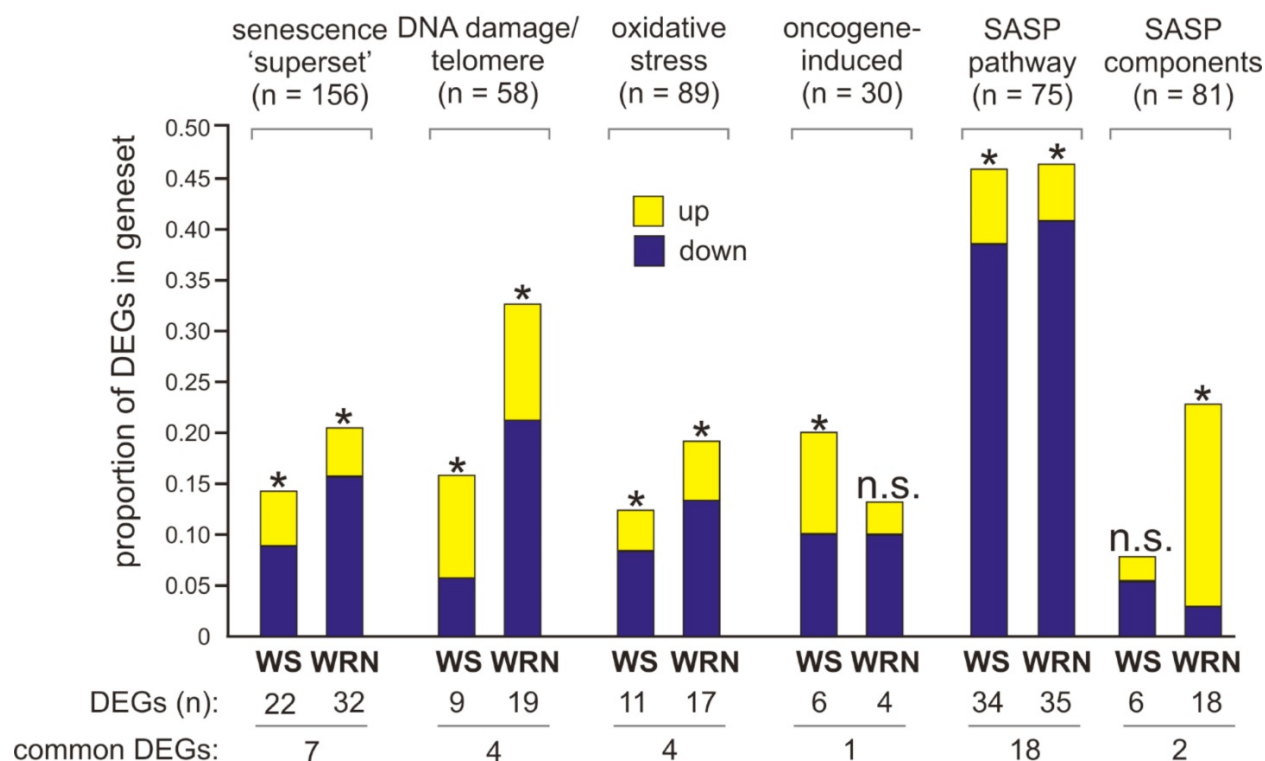
Fig. 4. WRN loss perturbs the expression of mechanistically distinct, senescence-associated genes and gene sets. Bar graphs indicate proportion of differentially expressed genes (DEGs) in senescence-associated gene sets in WS patient (WS) or WRN-depleted (WRN) cells. Gene sets and gene number/set are indicated over bars, with shading indicating increased (yellow) or decreased (blue) expression in WS or WRN-depleted fibroblasts. GSEA intersect p values of <0.05 are indicated by asterisks. Common DEGs were regulated in the same direction across all 6 gene sets.

Table 1. Ingenuity Pathways Analysis (IPA) summary

Werner syndrome (WS) fibroblasts
Top molecular/cellular functions

Function	p value	molecules
cellular growth/proliferation	3.8E-12	468
cell death/survival	7.2E-10	408
cellular development	2.0E-09	377
cell movement	3.5E-07	287
cell cycle	4.1E-07	180

WRN-depleted control fibroblasts

Function	p value	molecules
cell cycle	1.4E-21	260
cellular growth/proliferation	3.3E-21	494
cell death/survival	1.8E-19	472
cellular assembly/organization	1.1E-18	277
DNA replication/recomb/repair	1.1E-18	176

Top canonical pathways

Pathway	p value	ratio
tRNA charging	1.26E-07	14/35
EIF2 signaling	1.35E-04	22/121
integrin signaling	1.66E-04	29/183
JAK/TYK in IFN signaling	2.14E-04	8/23
AHR signaling	3.09E-04	22/128

Pathway	p value	ratio
AHR signaling	3.10E-08	30/140
cell cycle:G2/M reg	4.38E-06	14/49
polo-like kinase mitotic roles	9.65E-05	16/66
gap junction signaling	2.90E-05	26/155
IL6 signaling	5.29E-05	21/116

Table 2. Gene Set Enrichment Analysis (GSEA) summary.

MSigDB gene set collection	gene sets (n)	intersect p-value cutoff	significant gene sets (n)*		
			WS-NM	WRN-NS	common
C1: Chromosome position	300	5.00E-02	9	15	1
C2: CGP (chemical/genetic perturbation)	3254	1.00E-08	72	187	50
C2: CP (canonical pathways)	1268	5.00E-02	125	248	42
C3: MIR (microRNA targets)	214	5.00E-02	17	22	3
C3: TFT (transcriptional factor targets)	598	5.00E-02	113	65	8
C4: CGN (cancer gene neighborhoods)	424	5.00E-02	41	61	21
C4: CM (cancer modules)	428	5.00E-02	67	140	50
C5: BP (GO Biological Process Ontology)	790	5.00E-02	58	146	25
C5: CC (GO cellular component)	210	5.00E-02	19	57	7
C5: MF (GO molecular function)	380	5.00E-02	31	52	8
C6: Oncogenic signatures	189	5.00E-02	29	75	21
C7: Immunologic signatures	1910	5.00E-02	283	761	175

*GSEA results are reported in greater detail in Table S14. Gene set comparisons used differentially expressed genes identified in WS patient versus matched control donor fibroblasts (WS-NM), in WRN shRNA versus non-specific shRNA-depleted isogenic control fibroblasts (WRN-NS) or in both cell types (common).